Pergamon

Cement and Concrete Research, Vol. 26, No. 10, pp. 1567-1577, 1996

0008-8846/96 $15.00 + .00

PII S0008-8846(96)00137-8

A TWO-PHASE MODEL FOR PREDICTING THE COMPRESSIVE STRENGTH OF CONCRETE

C.C. Yang* and R. Huang**
* Institute of Materials Engineering
** Department of Harbor and River Engineering
National Taiwan Ocean University, Keelung, Taiwan, R. O. C.

(Refereed)
(Received April 19, 1996; in final form July 29, 1996)

ABSTRACT

In order to study the strength of concrete, cement-based composite material specimens with different volume fractions (10%, 20%, and 30%) of aggregate and two water/(cement+ silicafume) ratios (w/b=0.28 and 0.6) were cast and tested. Theoretical analysis was investigated in this study by employing the theory of micromechanics. A new approach is proposed to obtain the average stress fields of inhomogeneities and matrix by use of the equivalent inclusion method and the concept of Mori-Tanaka theory. The uniaxial compressive strength of cement-based composite materials can be considered as a function of component properties of composite, and the volume fraction of aggregate. The compressive strength of concrete is controlled by the weakest component. The comparison is also made between theoretical results and the experimental data.

Introduction

A composite can be defined as a combination of at least two different materials. Usually the properties of multiphase composite should be superior to the properties of the individual phase and may have different properties of the original components. It is appropriate to consider concrete as a cement-based composite which consists of coarse aggregate embedded in a matrix of hydrated mortar.

Aïtcin and Neville (1) pointed out that the strength of normal strength concrete is controlled by the strength of the hydrated cement paste based on their experiments. In high-strength concrete, the strength of concrete is controlled by the weakest component (2), and the fracture surfaces pass through the coarse aggregate as well as the cement pastes (3). Aïtcin and Mehta (4) demonstrated that the compressive strength of high-strength concrete is limited by the strength of the aggregate. Baklbaki et al. (2) and Tighiouart et al. (5) provided some experimental results for the strength of concrete with different aggregates and mortars. Giaccio et al. (6) demonstrated that the influence of aggregate characteristics on concrete strength increases in high-strength concrete.

The stress disturbance due to the inhomogeneity can be simulated by an eigenstress caused by an inclusion when the eigenstrain is chosen properly (7). Such equivalency was derived from the equivalent inclusion method. Mori and Tanaka (8) have applied the concept of average field to analyze the macroscopic properties of composite materials. The average field in a body contained inclusions with eigenstrain. In addition, the shape effect of dispersoids introduced in Eshelby's method (9) was applied to evaluate the properties of composite materials.

In this study, the strength of cement-based composites was obtained in the laboratory. A new approach was also made by employing micromechanics method to predict the compressive strength of concrete. In the theoretical model, concrete was considered as a two-phase composite and the bond between aggregate and matrix was assumed to be perfect. The average stress fields in mortar and aggregate were calculated and the compressive strength of concrete was controlled by the strength of the weakest component. Theoretical predictions was also compared with experimental data.

Experimental Program

In the experimental program, cement-based materials were made with different artificial aggregates and matrixes. The aggregates were made of portland cement paste. The composite specimens were cast and cured in the laboratory.

Aggregate. Artificial aggregates were cast using cement pastes with three water/cement ratios (w/c=0.4, 0.5, and 0.6). The artificial aggregates were cast in the spherical mold and cured in water until casting the composite specimens. Specimens without aggregates (ϕ 150 × 300 mm) were also cast and cured. At the age of 28 days, the elastic modulus and compressive strength of the composite specimens were determined according to ASTM C469-81 and ASTM C39-81, respectively.

TABLE 1
Mix Design (Kg/m^3)

	Mortar Phase, per m^3					Aggregate Phase, per m^3		
design -ation	water	cement	sand	silica-fume	s p	aggregate	W/C of aggregate	volume fraction (%)
341 351 361	209.7	692.5	996.9	59.8	15.7	226.6 210.6 202.6	0.4 0.5 0.6	10
342 352 362	186.3	615.3	871.8	53.2	13.9	453.2 421.2 405.2	0.4 0.5 0.6	20
343 353 363	162.9	538.1	1150.	46.5	12.2	679.8 631.8 607.8	0.4 0.5 0.6	30
641 651 661	360.5	553.3	896.1	47.8	0	226.6 210.6 202.6	0.4 0.5 0.6	10
642 652 662	320.3	491.6	796.2	42.4	0	453.2 421.2 405.2	0.4 0.5 0.6	20
643 653 663	280.1	429.9	696.3	37.1	0	679.8 631.8 607.8	0.4 0.5 0.6	30

TABLE 2
Properties of Aggregate, Matrix and Composite

design -ation	matrix				aggregate					composite
	w/b	E_m (GPa)	ν_m	f_m (MPa)	w/c	V_a (%)	E_a (GPa)	ν_a	f_a (MPa)	f_c (MPa)
341	0.28	24.81	0.22	66.36	0.4	10	18.06	0.21	53.24	61.57
342						20				60.30
343						30				58.14
351					0.5	10	15.43	0.20	40.09	52.13
352						20				47.72
353						30				45.30
361					0.6	10	13.96	0.20	29.72	41.70
362						20				38.63
363						30				35.94
641	0.6	15.71	0.20	34.22	0.4	10	18.06	0.21	53.24	33.18
642						20				33.35
643						30				33.98
651					0.5	10	15.43	0.20	40.09	35.66
652						20				34.61
653						30				33.77
661					0.6	10	13.96	0.20	29.72	29.34
662						20				28.28
663						30				27.56

Cement-Based Composite. Two water/(cement+ silicafume) ratios (w/c=0.28 and 0.6) and different volume fractions (a/t=0., 0.1, 0.2, and 0.3) of aggregate were considered in the mix proportions. The mix design of this investigation are given in Table 1.

Composite cylinders (ϕ 150 × 300 mm) were cast and cured. At the age of 28 days, the elastic moduli and compressive strength of the composites were measured according to ASTM C 469-81 and ASTM C 39-81, respectively. All the test results are the average of three specimens. The properties of aggregate, matrix and composite are shown in Table 2.

Theoretical Background

The relationship between the applied stress $\underset{\sim}{\sigma}^{o}$ and the properties of the constituent materials of the composite is determined using micromechanics method. The average stresses in the inhomogeneities, $\underset{\sim}{\sigma}^{o}+\langle\underset{\sim}{\sigma}\rangle_{\Omega}$, and in the matrix, $\underset{\sim}{\sigma}^{o}+\langle\underset{\sim}{\sigma}\rangle_{M}$, are derived based on the equivalent inclusion method (7). From the view point of the average stress fields, the strength of the composite is controlled by the weakest component so that the fracture propagates when the average stress fields in the component reach its ultimate strength.

Model. Considering there exist spherical inhomogeneities, $\Omega = \sum_{i=1}^{N}\Omega_i$, with elastic moduli $\underset{\sim}{C}^{*}$ and a volume fraction V_f randomly embedded in an infinite matrix with the stiffness $\underset{\sim}{C}$,

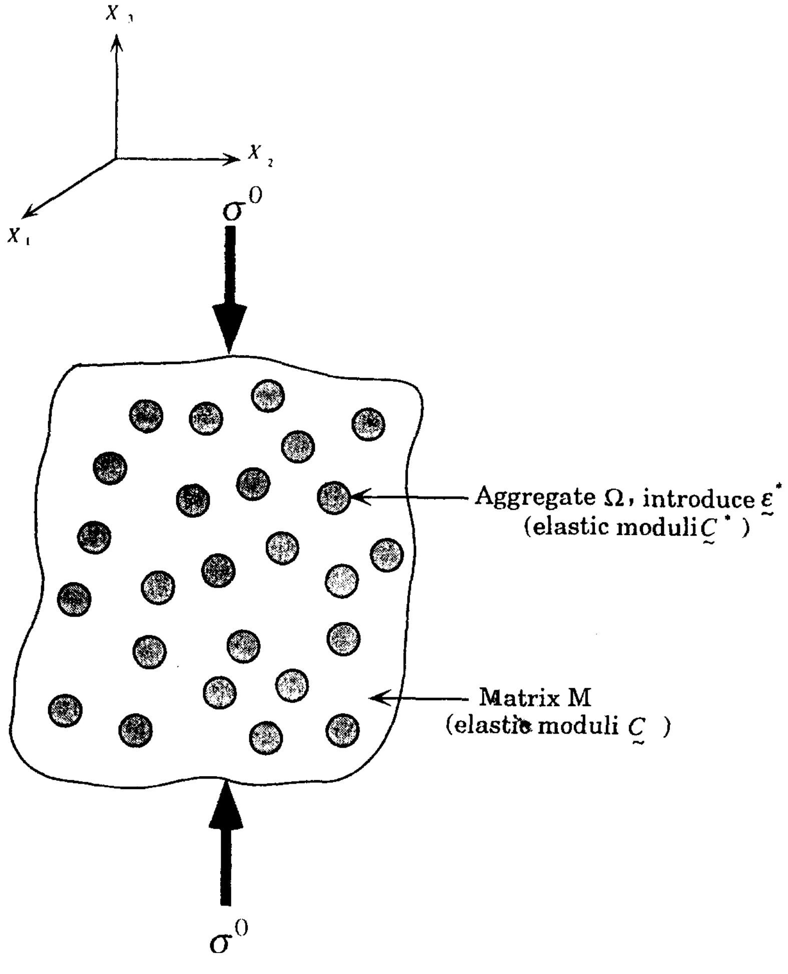

FIG. 1.
Spherical inclusions embedded in an isotropic infinite body under uniaxial compressive stress.

the stress disturbance in the applied compressive stress, $\underset{\sim}{\sigma}^o$, due to inhomogeneities can be simulated by the eigenstress caused by the fictitious misfit strain (Fig. 1). In this study, the fictitious misfit strain (eigenstrain), $\underset{\sim}{\varepsilon}^*$, was introduced to simulate the inhomogeneity effect. By use of the equivalent inclusion method (7) and represent Mori-Tanaka theory (8), the total stress in the inhomogeneity can be as follows

$$\underset{\sim}{\sigma}^o+\left\langle\underset{\sim}{\sigma}\right\rangle_\Omega=\underset{\sim}{C}\left\{\underset{\sim}{C}^{-1}\left(\underset{\sim}{\sigma}^o+\left\langle\underset{\sim}{\sigma}\right\rangle_M\right)+\left\langle\underset{\sim}{\Delta\gamma}\right\rangle-\left\langle\underset{\sim}{\varepsilon}^*\right\rangle\right\} \tag{1}$$

or

$$\underset{\sim}{\sigma}^{o}+\left\langle\underset{\sim}{\sigma}\right\rangle_{\Omega}=\underset{\sim}{C}^{*}\left\{\underset{\sim}{C}^{-1}\left(\underset{\sim}{\sigma}^{o}+\left\langle\underset{\sim}{\sigma}\right\rangle_{M}\right)+\left\langle\underset{\sim}{\Delta\gamma}\right\rangle\right\}, \tag{2}$$

where $\left\langle\underset{\sim}{\Delta\gamma}\right\rangle$ is the average disturbance strain caused by eigenstrain $\left\langle\underset{\sim}{\varepsilon}^{*}\right\rangle$ in a single inhomogeneity and related to $\left\langle\underset{\sim}{\varepsilon}^{*}\right\rangle$ by

$$\left\langle\Delta\gamma\right\rangle=\underset{\sim}{S}\left\langle\underset{\sim}{\varepsilon}^{*}\right\rangle. \tag{3}$$

Where $\underset{\sim}{S}$ is the Eshelby tensor for a single inclusion which solely exists in an infinite homogeneous medium. The Eshelby tensor is a function of the geometry of the inclusion and Poisson's ratio of the matrix (see appendix).

<u>Average Stress of Inclusions and Matrix</u>. The average of the stress disturbance $\underset{\sim}{\sigma}$ is zero (7), i.e.,

$$V_f\left\langle\underset{\sim}{\sigma}\right\rangle_{\Omega}+\left(1-V_f\right)\left\langle\underset{\sim}{\sigma}\right\rangle_{M}=0. \tag{4}$$

The average disturbance stress in the inhomogeneities, $\left\langle\underset{\sim}{\sigma}\right\rangle_{\Omega}$, are obtained by solving eqn (1) and eqn (3), i.e.,

$$\left\langle\underset{\sim}{\sigma}\right\rangle_{\Omega}=\left\langle\underset{\sim}{\sigma}\right\rangle_{M}+\underset{\sim}{C}\left(\underset{\sim}{S}-\underset{\sim}{I}\right)\left\langle\underset{\sim}{\varepsilon}^{*}\right\rangle, \tag{5}$$

where $\underset{\sim}{I}$ is the unit tensor. The second term in eqn (5), $\underset{\sim}{C}\left(\underset{\sim}{S}-\underset{\sim}{I}\right)\left\langle\underset{\sim}{\varepsilon}^{*}\right\rangle$, is the average stress field in the inclusion when only one inclusion is considered. The average stress in the inclusion is taken as the sum of the average stress in the matrix and the stress for a single inclusion. This corresponds to the basic assumption in Mori-Tanaka's theory.

Substituting eqn (5) into eqn (4), the average disturbance stress in the matrix, $\left\langle\underset{\sim}{\sigma}\right\rangle_{M}$, is calculated as

$$\left\langle\underset{\sim}{\sigma}\right\rangle_{M}=-V_f\underset{\sim}{C}\left(\underset{\sim}{S}-\underset{\sim}{I}\right)\left\langle\underset{\sim}{\varepsilon}^{*}\right\rangle. \tag{6}$$

Using eqns (5) and (6), the average disturbance stress in the inhomogeneities, $\langle \underset{\sim}{\sigma} \rangle_{\Omega}$, is rewritten as

$$\langle \underset{\sim}{\sigma} \rangle_{\Omega} = (1-V_f)\underset{\sim}{C}(\underset{\sim}{S}-\underset{\sim}{I})\langle \underset{\sim}{\varepsilon}^{*} \rangle. \tag{7}$$

Substituting eqns (6) and (7) into eqn (2) and solving for $\langle \underset{\sim}{\varepsilon}^{*} \rangle$, have

$$\langle \underset{\sim}{\varepsilon}^{*} \rangle = \alpha^{-1}(\underset{\sim}{C}-\underset{\sim}{C}^{*})\underset{\sim}{C}^{-1}\underset{\sim}{\sigma}^{o} \tag{8}$$

with

$$\alpha = (1-V_f)(\underset{\sim}{C}^{*}-\underset{\sim}{C})\underset{\sim}{S} - V_f(\underset{\sim}{C}-\underset{\sim}{C}^{*}) + \underset{\sim}{C} \tag{9}$$

Substituting eqn (8) into eqns (6) and (7). the average total stresses in the matrix and in the inhomogeneities are obtained as

$$\underset{\sim}{\sigma}^{o} + \langle \underset{\sim}{\sigma} \rangle_{M} = \left[\underset{\sim}{I} - V_f\underset{\sim}{C}(\underset{\sim}{S}-\underset{\sim}{I})\alpha^{-1}(\underset{\sim}{C}-\underset{\sim}{C}^{*})\underset{\sim}{C}^{-1}\right]\underset{\sim}{\sigma}^{o} \tag{10}$$

and

$$\underset{\sim}{\sigma}^{o} + \langle \underset{\sim}{\sigma} \rangle_{\Omega} = \left[(1-V_f)\underset{\sim}{C}(\underset{\sim}{S}-\underset{\sim}{I})\alpha^{-1}(\underset{\sim}{C}-\underset{\sim}{C}^{*})\underset{\sim}{C}^{-1} + \underset{\sim}{I}\right]\underset{\sim}{\sigma}^{o}. \tag{11}$$

Strength. The ultimate applied stresses in matrix and inhomogeneities ($\underset{\sim}{\sigma}_{m}^{o}$ and $\underset{\sim}{\sigma}_{\Omega}^{o}$) are obtained when the average stress reaches the strength of the matrix or inhomogeneities. If $\underset{\sim}{\sigma}_{m}^{o}$ is less than $\underset{\sim}{\sigma}_{\Omega}^{o}$, the composite strength $\underset{\sim}{f}_{c}$ is controlled by the matrix strength $\underset{\sim}{f}_{m}$. If $\underset{\sim}{\sigma}_{\Omega}^{o}$ is less than $\underset{\sim}{\sigma}_{m}^{o}$, the composite strength $\underset{\sim}{f}_{c}$ is controlled by the inhomogeneity strength $\underset{\sim}{f}_{a}$.

When the average stress in the matrix, $\underset{\sim}{\sigma}^{o} + \langle \underset{\sim}{\sigma} \rangle_{M}$, reaches the strength of matrix $\underset{\sim}{f}_{m}$, the ultimate applied compressive stress $\underset{\sim}{\sigma}_{m}^{o}$ can be obtained from eqn (10) and expressed as

$$\underset{\sim}{\sigma}_{m}^{o} = \left[\underset{\sim}{I} - V_f\underset{\sim}{C}(\underset{\sim}{S}-\underset{\sim}{I})\alpha^{-1}(\underset{\sim}{C}-\underset{\sim}{C}^{*})\underset{\sim}{C}^{-1}\right]^{-1}\underset{\sim}{f}_{m}. \tag{12}$$

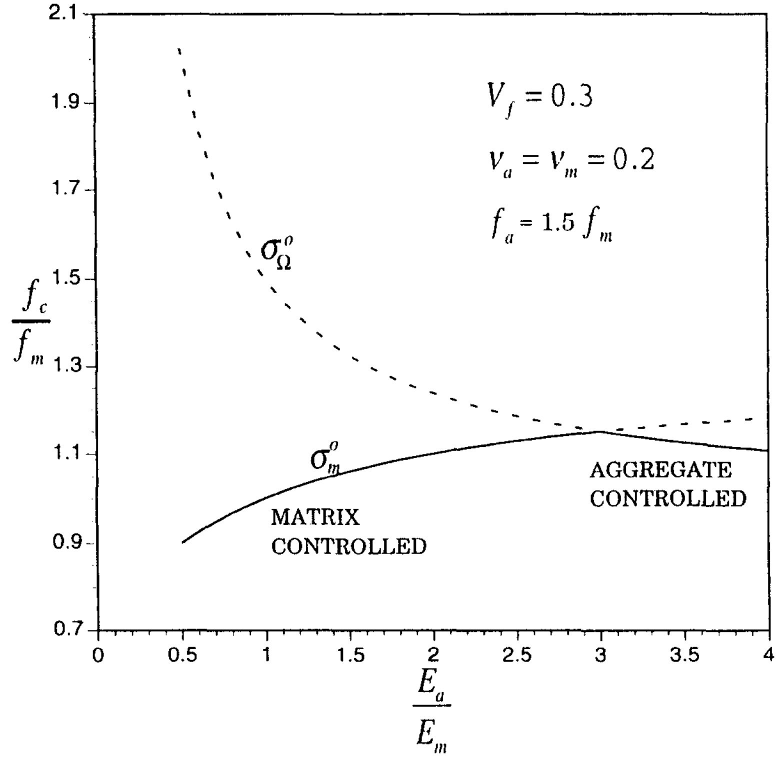

FIG. 2.

f_c/f_m vs. E_a/E_m curve $\left(f_a = 1.5 f_m\right)$

When the average stress in inhomogeneities, $\underset{\sim}{\sigma}^o + \left\langle \underset{\sim}{\sigma} \right\rangle_\Omega$, reaches the strength of inhomogeneities $\underset{\sim}{f_a}$, the ultimate applied compressive stress $\underset{\sim}{\sigma}^o_\Omega$ can be derived from eqn (11) and expressed as

$$\underset{\sim}{\sigma}^o_\Omega = \left[\left(1 - V_f\right)\underset{\sim}{C}\left(\underset{\sim}{S} - \underset{\sim}{I}\right)\alpha^{-1}\left(\underset{\sim}{C} - \underset{\sim}{C}^*\right)\underset{\sim}{C}^{-1} + \underset{\sim}{I}\right]^{-1} \underset{\sim}{f_a}. \tag{13}$$

Thus, composite strength $\underset{\sim}{f_c}$ is determined by $\underset{\sim}{\sigma}^o_m$ or $\underset{\sim}{\sigma}^o_\Omega$ whichever is smaller.

Results and Discussions

The Poisson's ratio for matrix and aggregate is 0.2 ($\nu_m = \nu_a = 0.2$) and volume fraction of aggregate is 0.3 ($V_f = 0.3$). A dimensionless parameter f_c/f_m is introduced. Figures 2 and 3

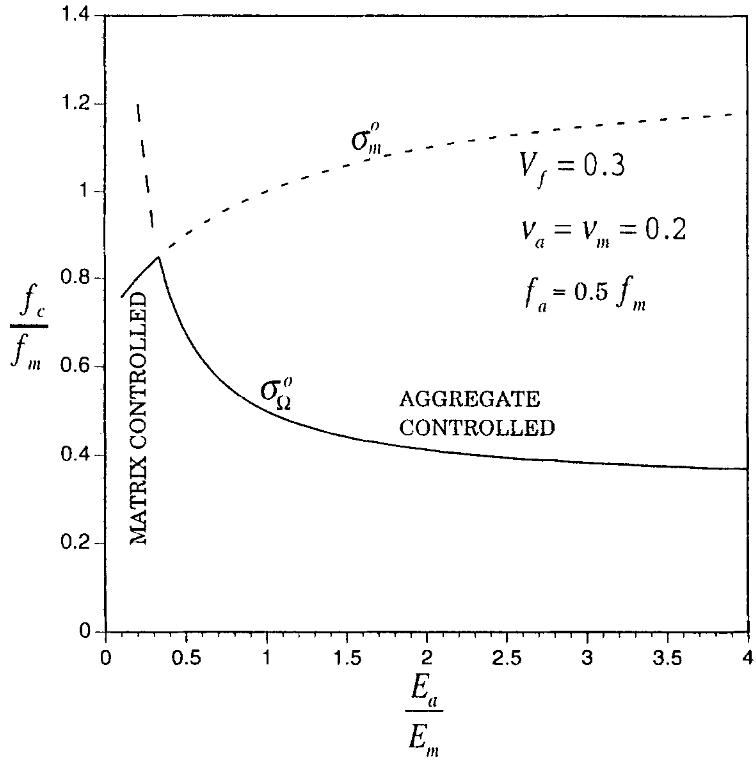

FIG. 3.

${}^{f_c}\!/\!_{f_m}$ vs. ${}^{E_a}\!/\!_{E_m}$ curve $(f_a = 0.5 f_m)$

show that the relationship between ${}^{f_c}\!/\!_{f_m}$ and ${}^{E_a}\!/\!_{E_m}$ (elastic modulus of aggregate/elastic modulus of matrix) for different aggregate strengths.

The effect of aggregate strength on the composite strength is illustrated in Figs. 2 and 3. When the ${}^{E_a}\!/\!_{E_m}$ ratio is less than 3 and f_a is equal to $1.5 f_m$, the strength of composite is controlled by the matrix strength. Consider that f_a (the strength of aggregate) is 1.5 times of f_m (the strength of matrix), and the ratio of ${}^{E_a}\!/\!_{E_m}$ is between 1 and 3, although the composite strength is controlled by matrix. However, the composite strength is higher than the matrix strength. In the case of $f_a < f_m$ as shown in Fig. 3, the composite strength decreases and the peak value of composite strength shifts to the left when the strength of aggregate decreases.

The experimental strength of cement-based composites were obtained from the test. The elastic moduli and Poisson's ratios of aggregate and matrix are presented in Table 2. From eqns (12) and (13), the applied stresses σ_m^o and σ_Ω^o are obtained when the average stress reaches the strength of the matrix and aggregate, respectively. If σ_m^o is less than σ_Ω^o, the composite strength is controlled by the matrix. If σ_Ω^o is less than σ_m^o, the composite strength

TABLE 3
Compressive Strength of Concrete, Measured and Calculated Values

designation	applied stress		concrete compressive strength		$\left(\frac{f_c^* - f_c^\#}{f_c^\#}\right) \times 100$
	σ''_m (MPa) Eq. (12)	σ''_Ω (MPa) Eq. (13)	f_c^* (MPa) (calculated)	$f_c^\#$ (MPa) (measured)	(%)
341	65.30	62.31	62.31	61.57	1.20
342	64.25	61.30	61.30	60.30	1.66
343	63.19	60.30	60.30	58.14	3.72
351	64.79	51.30	51.30	52.13	-1.59
352	63.22	50.06	50.06	47.42	5.57
352	61.64	48.81	48.81	45.30	7.75
361	64.48	40.30	40.30	41.70	-3.36
362	62.60	39.13	39.13	38.63	1.29
363	60.72	37.95	37.95	35.94	5.59
641	34.47	50.01	34.47	33.18	3.89
642	34.72	50.37	34.72	33.35	4.11
643	34.96	50.72	34.96	33.98	2.88
651	35.73	40.42	35.73	35.66	0.20
652	35.70	40.38	35.70	34.61	3.15
653	35.66	40.34	35.66	33.77	5.60
661	35.55	31.62	31.62	29.34	7.77
662	35.34	31.43	31.43	28.28	11.14
663	35.13	31.24	31.24	27.56	13.35

is controlled by the aggregate. The comparisons of analytical compressive strength and the experimental results of the cement-based are displayed in Table 3. The theoretical predictions have a fair agreement with the experimental results.

TABLE 4
The Mechanical Properties of Mortars and Aggregates

author [year]	aggregate type	aggregate				mortar			
		E_a (GPa)	ν_a	f_a (MPa)	V_f (%)	w/c	E_m (GPa)	ν_m	f_m (MPa)
Baalbaki et al. [1991]	quartzite	42	.16	96	40.0	.27	38	.20	108
	limestone	49	.14	115	40.0	.27	36	.20	106
	sandstone	40	.10	147	40.0	.27	38	.20	108
Tighiouart et al. [1994]	limestone	68	.16	295	37.5	.50	30	.18	45.1
	granite	66	.10	220	38.6	.50	30	.18	45.1
	quartzite	44	.14	87	38.6	.50	30	.18	45.1
	sandstone	37	.08	205	41.5	.50	30	.18	45.1
	limestone	68	.16	295	37.5	.27	39	.18	88.6
	granite	66	.10	220	38.6	.27	39	.18	88.6
	quartzite	44	.14	87	38.6	.27	39	.18	88.6
	sandstone	37	.08	205	41.5	.27	39	.18	88.6
	limestone	68	.16	295	37.5	.22	42	.18	104.6
	granite	66	.10	220	38.6	.22	42	.18	104.6
	quartzite	44	.14	87	38.6	.22	42	.18	104.6
	sandstone	37	.08	205	41.5	.22	42	.18	104.6

TABLE 5
Compressive Strength of Concrete, Measured and Calculated Values

aggregate type	mortar W/C	applied stress σ''_m (MPa) Eq. (12)	σ''_Ω (MPa) Eq. (13)	concrete compressive strength f'_c (MPa) (calculated)	$f^{\#}_c$ (MPa) (measured)	author [year]
quartzite	0.27	110	94	94	99	Baalbaki
limestone	0.27	112	107	107	106	et al.
sandstone	0.27	108	147	108	107	[1991]
limestone	0.50	51.7	243.5	51.7	56.2	
granite	0.50	51.4	184.2	51.4	59.5	
quartzite	0.50	48.3	78.8	48.3	53.4	
sandstone	0.50	46.7	196.1	46.7	57.2	
limestone	0.27	97.5	255.9	97.5	92.1	Tighiouart
granite	0.27	96.9	193.8	96.9	100.3	et al.
quartzite	0.27	90.4	84.4	84.4	93.4	[1994]
sandstone	0.27	87.0	211.6	87.0	113.3	
limestone	0.22	113.8	260.1	113.8	117.2	
granite	0.22	113.0	197.0	113.0	127.4	
quartzite	0.22	105.2	86.3	86.3	103.3	
sandstone	0.22	101.1	216.7	101.1	118.8	

By reviewing the previous study (2, 5), the experimental results of the concrete compressive strength with different aggregates (quartzite, limestone, granite, and sandstone) were reported by Baalbaki et al. (2) and Tighiouart et al. (5). The aggregate volume fraction ranged from 37 percent to 40 percent and the water/cement ratios were 0.20, 0.27, and 0.5. Table 4 shows the mechanical properties of mortar and aggregates. The aggregates specimens (ϕ 52 × 104 mm) were cored from intact rectangular blocks. The mechanical characteristics of aggregates were determined according to ASTM D 2938 for compressive strength and ASTM D 3148 for elastic modulus and Poisson's ratio. The size of specimens used for concrete compressive strength tests at 91 days was ϕ100 × 200 mm and for mortar was ϕ52 × 104 mm. Tables 5 display the comparisons between the analytical compressive strengths and the experimental results.

It appears that the calculated compressive strengths agree fairly with the experimental results. The shape effect is not taken into account in the analytical procedure.

Conclusions

A theoretical approach for estimating the compressive strength of concrete composite materials is proposed by considering concrete as a two-phases composite (it assumes that the bond is perfect between mortar and aggregate). Based on the theoretical predictions and experimental results, the compressive strength of concrete is mainly influenced by the properties and the volume fraction of aggregate. The compressive strength of concrete is not always limited by the strength of its components; the concrete strength may be higher than the strength of its components (see Fig. 2 and Fig. 3). When the effect of maximum aggregate size is not accounted for, the theoretical predictions are fairly close to the experimental results even if the shape effect of aggregate is not taken into account. This study is an initiation to apply micromechanics on the strength of concrete. More extensive and more refined researches need to be done to consider the failure of transition zone.

Acknowledgment

The financial support of National Science Council, ROC, under the grants NSC 84-2211-E-019-009 is gratefully appreciated.

Appendix

The Eshelby's tensor $\underset{\sim}{S}$ for sphere inclusion is listed below (7).

$$S_{1111} = S_{2222} = S_{3333} = \frac{7 - 5\nu}{15(1 - \nu)}.$$

$$S_{1122} = S_{2233} = S_{3311} = S_{1133} = S_{2211} = S_{3322} = \frac{5\nu - 1}{15(1 - \nu)}.$$

$$S_{1212} = S_{2323} = S_{3131} = \frac{4 - 5\nu}{15(1 - \nu)}.$$

References

1. P.C. Aïtcin, and A. Neville, Concrete International, 15, 21 (1993).
2. W. Baalbaki, B. Benmokrane, O. Chaallal, and P. C. Aïtcin, ACI Mat. J., 88, 499 (1991).
3. S.L. Sarkar, and P.C. Aïtcin, ASTM, STP 1061, 129 (1990).
4. P.C. Aïtcin, and P.K. Mehta, ACI Mat. J., 87, 103 (1990).
5. B. Tighiouart, B. Benmokrane, W. Baalbaki, Mat. and Stru., 27, 211 (1994).
6. G. Giaccio, C. Rocco, D. Violini, J. Zappiteelli, and R. Zerbino, ACI Mat. J., 89, 242 (1992).
7. T. Mura, Micromechanics of Defects in Solids, Second Revised Edition, Martinus Nijhoff Publishers, 1987.
8. T. Mori and K. Tanaka, Acta Metall., 21, 571 (1973).
9. J.D. Eshelby, Proc. Roy. Soc., A241, 376 (1957).